Experimental study of liquid movement in free elementary convective cells

Liudmyla Bozbiei[1, 3]**,**

Boris Borts[1]**,**

Yuri Kazarinov[1]**,**

Andrey Kostikov[2, 3]**,**

Viktor Tkachenko[1, 2]

[1] *National Science Center*
Kharkov Institute of Physics and Technology,
National Academy of Sciences of Ukraine,
Akademicheskaya St. 1, 61108,
Kharkov, Ukraine
E-mail tkachenko@kipt.kharkov.ua

[2] *V. N. Karazin Kharkiv National University,*
Svobody Sq. 4, 61022, Kharkov, Ukraine

[3] *A. N. Podgorny Institute*
for Mechanical Engineering Problems,
National Academy of Sciences of Ukraine,
Pozharsky St. 2/10, 61046, Kharkov, Ukraine

Elementary convection cells (ECC) are formed in horizontal layers of liquid heated from below, and they are experimentally investigated in this work. Results of experimental studies were adequately described by the theoretical model of ECC. It is shown that the addition of aluminum powder to oil transforms oil to a suspension, such that boundary conditions on the solid wall can be regarded as free because there is a slip through the tape of pure oil. Change in the character of boundary conditions is confirmed by the results of numerical processing of experimental results on formation of convective rings on the layer surface by other authors. Two independent methods for determining the velocity of mass transfer in cells with various diameters are described in the article. For cells with a large diameter (17 mm), the maximum velocity of mass transfer was measured at the upper boundary on a deflection angle of the probe. Measured in this way velocity was equal to $V_{Oil} \approx 0.2$ mm/sec. For cells with a smaller diameter (2 mm), the velocity of oil on the surface of a cell was measured using an optical method and constituted the value from 3.5 mm/s to 5.2 mm/s.

Key words: elementary convective cell, convective processes, transfer of heat, temperature gradient, velocity of mass transfer in the cell

INTRODUCTION

Numbers of articles, reviews and monographs were devoted to the study of convective processes in a horizontal layer of incompressible, viscous fluid heated from below. They include early experimental and theoretical papers [1, 2], and later, but very informative papers, monographs and reviews on the subject [3–6].

In work [7], it has been suggested that the energy principle can be a fundamental principle of formation of polygonal convective structures in a temperature tense medium rather than a geo-metric principle referred to above. The energy principle associates the quantity, size and shape of convection cells with the magnitude of the temperature gradient inside a cell and the temperature of a vessel at the bottom. In accordance with this, it is asserted that with the increase of temperature of the bottom of the vessel in liquid, secluded (discontiguous) cylindrical convective elementary cells (ECC) appear first, the number of which with the increase of the temperature becomes so great that they become tightly packed and fill in the entire volume of a liquid vessel and thus form polygonal convective cells.

Horizontal and vertical velocity components of ECC are described by Bessel functions of the first kind of the zero order and the first order, respectively. It should be noted that the physical properties of the proposed ECC correspond to the experimental data on the convection of liquid in small containers heated from below [8].

The purpose of this work is to prove the existence of an elementary convective cell by comparing the theoretical model and experimental data as well as the experimental determination of characteristic velocities of fluid heat convection inside a cell.

SOLUTION OF THE RAYLEIGH PROBLEM IN A CYLINDRICAL COORDINATE SYSTEM

The perturbed velocity of convective mass transfer and distribution of the temperature in a horizontal layer in a viscous, incompressible fluid heated from below are described by Navier-Stokes equations in the Boussinesq approximation. In cylindrical geometry, the dimensionless perturbations of velocity $\vec{v}$ and the temperature T in dimensionless variables t, r, z have the form [7]:

$$v_z(r, z, t) = A\sin(n\pi z)\, J_0(k_r\, r)\, \exp(-\lambda t), \qquad (1)$$

$$v_r(r, z, t) = An\pi k_r^{-1}\cos(n\pi z)\, J_1(k_r r)\, \exp(-\lambda t), \quad (2)$$

$$T(r, z, t) = B\sin(n\pi z)\, J_0(k_r r)\, \exp(-\lambda t), \qquad (3)$$

where the axis of z is directed upward and perpendicular to the layer boundaries $z = 0$ and $z = 1$; $n = 1, 2, 3,\ldots$ are integers that correspond to perturbation modes; A and B are constant coefficients; λ are eigenvalues of the system that characterize attenuation ($\lambda = 0$), increase ($\lambda = 0$) or the stationary state ($\lambda = 0$) of perturbations (1)–(3); $J_0(x)$ and $J_1(x)$ are Bessel functions of the first kind of zero and the first order, respectively; k_r is the radial wave number that characterizes dependence of perturbations on the transverse coordinate r.

For non-dimensional expressions (1)–(3), such characteristic dimensional parameters of the problem as layer thickness h, time $\tau = h^2\nu^{-1}$, speed $\tau = h^2\nu^{-1}$, temperature $\Theta = T_2 - T_1 > 0$, pressure $\rho_0\nu\chi h^{-2}$, where T_2 and T_1 are temperature of upper and lower boundaries of a layer, respective-

ly, where ν and χ are kinematic viscosity and thermal diffusivity of fluid, are used.

Solutions (1)–(3) are valid for a convective cell with free boundary conditions, when tangential stress and perturbation of temperature at the layer boundaries at $z = 0$ and $z = 1$ are equal to zero. It is then:

$$v_z\big|_{z=0;1} = 0, \frac{\partial^2 v_z}{\partial z^2}\bigg|_{z=0;1} = 0, T\big|_{z=0;1} = 0. \qquad (4)$$

The characteristic time for typical oil is in the order $\tau = h^2/\mu_{Oil} = 0.1\ldots.0.01$ s, where $h = 1$ mm, viscosity of vacuum oil and its analogs at the temperature of 100 °C is $\mu^{VM}_{Oil} = 8-11$ mm²/s [7, 9], and silicone oil at the temperature of 25 °C is $\mu^{S}_{Oil} = 100$ mm²/s [8]. Experimentally observed stable existence of a cylindrical cell for a quite long interval of time (more than 100 sec) and a balance of its perturbation exponential factor $\exp(-\lambda(t/\tau))$, where characteristic time τ is sufficiently small, inevitably lead to the conclusion that the eigenvalues λ must equal zero or λ must be close to zero. Therefore, we will consider only stable solution of (1)–(3) in the sequel when $\lambda = 0$.

In decisions (1)–(3), the radial wave number k_r remains an indefinite parameter. Its value is determined from the condition of the zero horizontal velocity v_r on the outer boundary of a convective cell. This condition sets the value of the radial wave number:

$$k_r = \sigma_{1,i}R_c^{-1}, \qquad (5)$$

where R_e is the radius of a convective cell that is divided by the depth of the layer, $\sigma_{1,i}$ is the i-th zero of the Bessel function of the first order ($J_1(\sigma_{1,i}) = 0$), $i = 1,2,3,\ldots$. In particular, the first zeros of the Bessel functions have the following meanings [10]: $\sigma_{1,1} = 3.832$; $\sigma_{1,2} = 7.016$; $\sigma_{1,3} = 10.173$.

It should be noted that solution (5) was previously presented in [11–13]. In these papers, current lines were constructed, and an axially symmetrical arrangement of concentric convective rolls for free upper boundaries and free lower boundaries of the solid (asymmetric boundary conditions) of a liquid layer was analysed. In particular, as follows from work [12], the radial wave number is defined by the ratio of the critical wave number $a = 2.682$ of the problem with asymmetric

boundary conditions (the notation of the cited work is kept) to the depth of the layer: $k_r = \dfrac{a}{h}$. In works [12, 13], values of critical wave numbers and their associated critical Rayleigh numbers for two other kinds of boundary conditions – two free boundaries and two rigid boundaries – are also shown. It is shown that the value of the radial wave number for every type of boundary conditions is determined by the critical wave number a of the corresponding type of boundary conditions ($a = 2.22$ – two free boundaries, $a = 3.13$ – two solid boundaries). Based on the foregoing, one can conclude that authors of these quoted works have not fully analysed decisions and determined the radial wave number, which in this case is given by condition (5).

SUBSTANTIATION OF FREE BOUNDARY CONDITIONS FOR RAYLEIGH PROBLEM

In order to substantiate the applicability of descriptions of the experimental data on formation of the elementary convection cell by a theoretical model, it is assumed that boundary conditions are free, taking into account the following considerations.

In experiments, a small amount (by volume) of aluminum pigment powder PAP-1 is added in vacuum oil, which represents finely divided plate shape aluminum particles; the average thickness of lobes is about 0.25–0.50 microns; the average linear dimensions are 20–30 microns. The bulk density of the powder is equal to 0.15–0.30 g/cm³ (GOST 5494-95).

As in the experiments the oil temperature varies in the ranges 100–150 °C, then the thickness of its surface layer at the lower boundary vessel is estimated to be about 0.25–0.35 mm [14], and is comparable to the thickness of aluminum petals. The thickness of the surface layer oil on the surface petals of aluminum is of the same order. The estimate shows that the average distance between the particles of aluminum constitutes the order of 10 microns, and is significantly greater than the thickness of the oil tape.

Under experimental conditions, oil (0.7–2.5 ml) with the addition of small amounts of aluminum pigment powder (58–65 mg) constituted a stable (non-coagulating) suspension during the long-time interval with the density exceeding the den-

sity of pure oil by an amount of order 5%. The dynamic viscosity of suspension, according to work [15], is proportional to the viscosity of pure oil. The dynamic viscosity of suspension, measured by the Stokes method, is less than the viscosity of pure oil by 1%.

From the foregoing one can conclude that there are two phases of liquid: pure oil, concentrated on the bottom of the vessel in a form of a surface layer, and suspension of particles of aluminum powder distributed in oil, which has different density and dynamic viscosity than that of pure oil.

Thereby, the suspension which is close to the bottom of the vessel can be considered as a separate, relatively denser than the pure oil dispersion medium, which moves on an oil substrate of a pure oil without friction, i. e. slipping [16]. In this sense, boundary conditions of a liquid layer can be considered as free.

INTERPRETATION OF CYLINDRICAL CONVECTIVE RINGS BY SOLUTION FOR ELEMENTARY CONVECTIVE CELLS WITH FREE BOUNDARIES

In paper [8], results of studies of formation of concentric convective rolls in a layer of silicone oil heated from below are presented. A small amount of aluminum powder was added for visualization of convective motion in oil, without noting any changes in oil properties and boundary conditions.

An interpretation of the conducted experiments [8] on formation of concentric convective rings in silicone oil with the addition of the necessary amount of aluminum powder will be presented below. Solutions (1)–(3) for free convective cells are used for this, as some amount of aluminum powder is added in oil, and boundary conditions can be considered as free. In this case, as mentioned above, suspension is formed in oil, which is different in density and viscosity from the pure oil. Under such conditions, it is considered that the surface tape of pure oil on a solid lower boundary will provide slippage of the suspension relatively to the bottom of the vessel, i. e. elimination of shear stresses. In this case, boundary conditions of a liquid layer can be regarded as free.

Figure 1 shows the examples of digitally processed and optimized images of convective concentric rings presented in work [8].

Let us present a brief description of these pictures.

In the center of the vessel (Fig. 1d), the flow is directed upward, i. e. here a large point of light of aluminum powder is formed, which is brought to the surface by an upward flow of oil. Further, light concentric rings of aluminum powder are observed over the radius, which are alternated with dark stripes in one. Light rings correspond to the rising flows of oil, and dark rings between them correspond to the downward flow.

It should be noted that the mechanism of formation of concentric thin light rings of aluminum powder is similar to the mechanism of formation of wind-streaks of sea foam, fragments of algae, phytoplankton and zooplankton, air bubbles in the formation of Langmuir circulation over water surface [17], with the only difference that particles of aluminum powder are heavier than oil and are kept afloat its upward flow.

In Fig. 1b, c in the center of the vessel, the flow is directed down, as the light point of aluminum powder has smaller sizes compared to Fig. 1d, due to the fact that not the full mass of aluminum powder can be captivated downwards by

downstream flow of the oil. Further on the radius, the same location sequence of concentric thin light rings of aluminum powder and dark stripes as that in the previous figure is observed.

The above described figures, constituting current lines at the border $z = 1$, were digitized and smoothed along the radius from the center of the vessel to its boundary, situated at the distance $R_0 = 10$ cm from the center. Dependencies of oil surface brightness in the vessel along its radius are shown with a solid line in Fig. 1. In Figure 1a $m = 13$, in 1b $m = 12$, in 1c $m = 10$, and in 1d $m = 9$ correspond to the visually determined number of convective rolls in a cell. In Fig. 1 b, c, d small peaks, which correspond to the thin light rings in the images on the right, are shown on curves in solid lines. These small peaks correspond to the movement of oil upwards. Consequently, in the vicinity of these small peaks (minima in the base curve), oil moves up. Among the marked minima of the base curve, there is another minimum, which corresponds to the motion of oil downwards (1–3).

The obtained solution (2) if $z = 1$ was used to describe the formed convective rolls on the surface of oil in the cylindrical vessel. To compare this solution to the experimental data from its radial dependence, the function $\Psi(r) = \sqrt{rJ_1\left(\dfrac{\pi}{w}r\right)}$
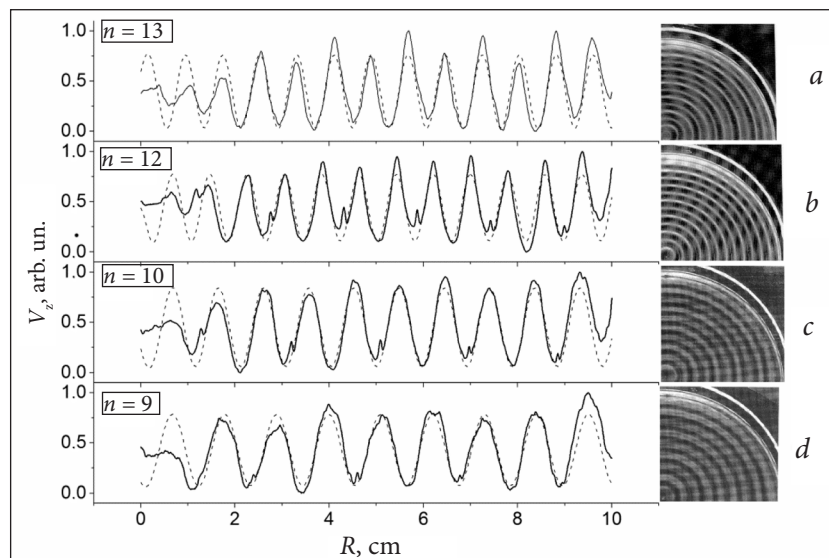
Fig. 1. Curves of numerical processing images of convective concentric rings (solid lines) and their optimization using results of the theoretical model (1)–(3) (dashed curves). The first quadrant of pictures of concentric rings, presented in work [8], is shown on the right side

was built that on multiplication by $\sqrt{r}$ describes streamlines (Stokes lines) in a cell at the border $z = 1$. The fittings of the function $\Psi(r)$ (dashed lines) to the experimental data showed a good quantitative correspondence of the theoretical model to the experiment. The view of the adjustment curve and coefficients of fitting are shown in Table 1.

As it follows from Fig. 1, the minima of curves of the digital processing correspond to the dark rings, which are consistent either with rising oil flows (marked by peaks of a small amplitude), or downward oil flows, located between the ascending. Figure 1 shows that the number of light rings equals $m = 9, 10, 12, 13$. Another dark ring corresponds to them.

Under large radii of rings in the fitting curve, the multiplier of the argument of the Bessel function $\frac{\pi}{w}$ can be represented in the form of $\frac{\sigma_{1,m}}{R_m} \approx \frac{2m\pi}{R_m}$, where R_m is the radius of m-th ring at the wall of the cylindrical container. As it follows, $R_m \approx 2mw$ corresponds to the location of light rings at the presented fragments of the images.

Thus, for example, as it follows from Table 1 and Fig. 1, for the value $m = 9$ the value of light ring radius is about $R_9 \approx 18 \cdot 0.55148 \approx 9.93$ cm, and it is situated almost near the wall of the vessel. For values $m = 10, 12$, radii of light rings equal $R_{10} \approx 20 \cdot 0.47989 \approx 9.6$ cm and $R_{12} \approx 24 \cdot 0.39478 \approx 9.47$ cm, and they are slightly removed from the wall of the vessel.

It should be noted that on the depth layer of oil 0.765 cm [8], estimation of the first ring radius in Fig. 1 constitutes about 1.3 cm. Based on this,

the diameter of the first ring in the depth units of the oil layer is equal to 3.4, which corresponds to the theoretically calculated value of the diameter of free convection cells [7].

The obtained results show that the layer of a viscous incompressible fluid with addition of aluminum powder and mixed boundary conditions with sufficient accuracy are described by analytic expressions for the same layer, but with free boundary conditions, due to the formation of two-phase medium in oil: suspension with different density and viscosity than that of the pure oil and pure oil in the form of a surface tape on the solid boundary.

Thus, in this chapter of the work, the results of experimental numerical processing and results of other authors on formation of convective rings in the layer of fluid heated from below confirm the assumption about changes of the character of boundary conditions from mixed (upper boundary is free, bottom limit is solid) to free.

FORMATION OF CONVECTIVE ISOLATED CELLS IN A COPPER RING, WHICH IS IMPOSED ON THE SURFACE OF OIL

Vacuum oil VM-5 (2 ml) was used in the experiments on research of properties of secluded convective cells, which are formed in oil. The thickness of the oil layer was 1.0–1.2 mm. Heating of the oil was conducted from the bottom by means of the electric furnace, and the temperature of the bottom of the vessel was kept at 135 ± 1 °C.

Experiments were performed in the following way. At first, Benard cells were formed in oil.

Table 1. **Parameters of the fitting curve and coefficients of fitting**

$$y = y_0 + a \cdot \sqrt{(r - r_0)} \cdot \left(\frac{\pi}{w} (r - r_0) \right)$$

Parameters of fitting	m = 9		m = 10		m = 12		m = 13	
	Value	Error	Value	Error	Value	Error	Value	Error
y_0	0.43042	0.00289	0.45206	0.00268	0.44015	0.00351	0.39752	0.00441
a	−1.06379	0.01232	−1.26018	0.0125	−1.17787	0.01839	1.29329	0.02337
r_0	−0.08269	0.00595	−0.15245	0.00407	−0.00673	0.00517	−0.12514	0.00639
w	0.55148	5.8017E-4	0.47989	3.4036E-4	0.39478	3.4223E-4	0.39334	4.132E-4

Further rings with different diameters made from copper wires 0.5 mm in thickness were imposed on the surface of oil with Benard cells. The diameter of the copper ring varied from 3 mm to 11 mm, with the step $l = 1$ mm. The experiments showed that the diameter of the resulting convective cell depends on the diameter of the copper ring in the step function (Fig. 2). As a result of each overlay of the copper ring with the diameter that increases step by step, the occurrence of the cylindrical convection cell, whose form is given in Figs. 3–10, was observed.

Pictures of convective cells, which are formed in copper rings, overlaid on the surface of the oil are shown in Figs. 3–10.

From the images presented in Figs. 3–10, one can conclude that upon the overlay of the ring on the surface of oil, different types of cells ap-

pear. Figures 3–4 show that overlay of the copper ring with less than 5 mm diameter results in the formation of the cell with the distribution of velocities of types (1), (2), where $m = 2$, i. e. two convective cells arranged one over another are formed. Thus, the relation of the diameter to the height of the cell should be about 3:1. The estimates show that the depth of the oil layer 1.0–1.2 mm allows realizing this arrangement of cells.

The increase of the diameter of the ring to a certain size (up to 5 mm) does not violate the size of the observable cell $D_c = 2.5$ mm. It supports the assumption of forming two cells, arranged one over another. Otherwise, upon formation of one cell ($m = 1$), the increase in the diameter of the cell should be observed with the increase of the diameter of the ring.
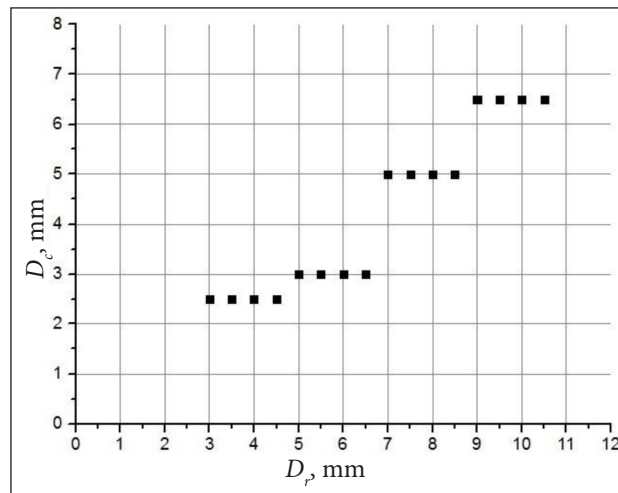
Fig. 2. Dependence of the diameter of the cell D_c on the diameter of the ring D_r
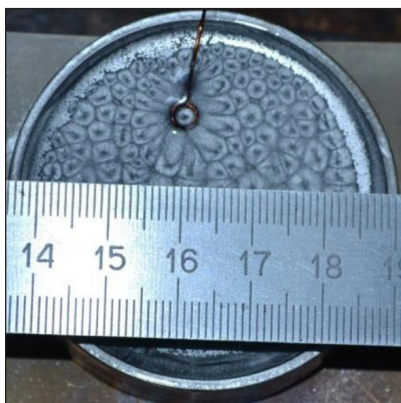
Fig. 3. $D_r = 3$ mm, $D_c = 2.5$ mm
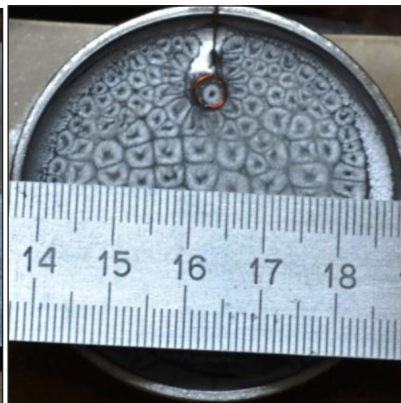
Fig. 4. $D_r = 4$ mm, $D_c = 2.5$ mm
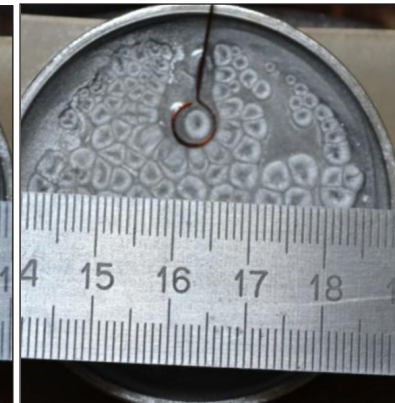
Fig. 5. $D_r = 5$ mm, $D_c = 3$ mm
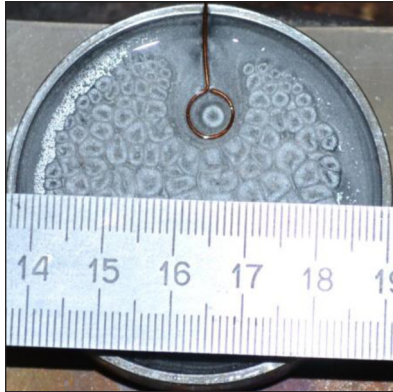
Fig. 6. $D_r = 6$ mm, $D_c = 3$ mm
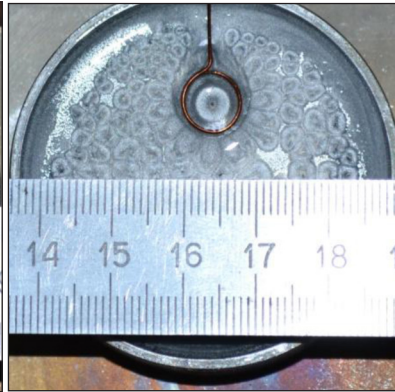
Fig. 7. $D_r = 7$ mm, $D_c = 5$ mm

Fig. 8. $D_r = 8$ mm, $D_c = 5$ mm

Excess of the ring size more than 5 mm will result in an intermittent increase of the size of the convective cell to the value of about 3 ± 0.5 mm. This confirms the formation of an elementary cell of type (1), (2) with $n = 1$ and diameter $D_c \approx 0.9 \cdot \sigma_{1.1}$ [7].

Fig. 9. $D_r = 9$ mm, $D_c = 6.5$ mm

Fig. 10. $D_r = 10$ mm, $D_c = 6.5$ mm

With the excess of the copper ring diameter 7 mm, the value of the cell diameter increased to about 5 mm and remained constant. Figures 7, 8 demonstrate the formation of the dark ring on the periphery of the cell, which corresponds to the formation of the convective ring, similar to the one observed in works [11–13].

Further increase of the ring radius (more than 9 mm) results in the formation of three convective cells inside the copper ring, and, for this case, the research of formation of elementary convective cells in the copper ring was not carried out.

Thus, in experiments on the formation of the cylindrical convective cell with overlay of the copper ring, a qualitative and quantitative correspondence of the theoretical model to the experimental data was presented.

MEASUREMENT OF VELOCITY OF MASS TRANSFER IN A CONVECTIVE CELL

One of the main questions that arise in the study of properties of Benard cells is the question of the value of velocity of convective mass transfer in a cell. Knowledge of the mathematical definition of velocity components in a cell (1)–(3) allows experimental determination of the true value. It is enough to measure the velocity of the horizontal mass transfer (2) on the surface of a cell at a point of its maximum value, i. e. under $r_* \approx R_c \cdot \sigma_{0.1}/\sigma_{1.1}$.

In order to measure the velocity of convective flow, series of experiments were conducted. Heating of oil was carried out from below by an electric furnace. Oil temperature was maintained at 150 ± 1 °C at the bottom of the vessel. In one of

the formed oil cells with a size of 17 mm, on top of the radius r_*, a probe made of two parallel thin cylindrical wires of copper with the diameter $d_w \approx 0.04$ mm was vertically lowered. The length of one wire was equal to $l = 4.3$ mm, and the length of the other wire was equal to $l = 5.4$ mm. Wires were fixed in a metal rod, which was located on a protractor to determine the angle of deflection of the longer wire to the relatively short one during its immersion into oil. Angles of deflection were fixed in accordance with Figs. 11–12.

Figure 12 shows that after immersion of the probe in the convection cell at radius r_* the angle of deflection of about $1 \pm 0.5°$ appears. In order to determine the velocity of mass transfer in a cell on the angle deflection value, it is necessary to calibrate the long wire of the measuring device.

Calibration of the long probe was carried out in a vertical jet of water, which flows free from a tap. To simplify the calibration procedure, water was chosen. Regulating flow of water from the tap with a valve, and measuring the diameter of the water jet, the mass of water and time of its expiration, and the velocity of water flow V_V can be determined from the formula:

$$V_V = \frac{4M}{\pi d^2 \rho t},$$ (6)

where M is the mass of water fallen into the measuring tank, d is the diameter of the water jet, ρ is the density of water, t is the time of water leakage into the tank.

Speed of water leakage from the tap, calculated according to formula (6), corresponded to the angle of the long wire deflection, introduced into the jet perpendicular to the cylindrical surface creating it.

The experimental data on the measurement of dependence of the wire deflection angle on the water velocity are presented in Table 2.

In order to describe the analytic dependence of the probe deflection angle from the water flow velocity, it is assumed that the probe is of a cylindrical shape. In this case, the probe resistance force to the oncoming water flow per unit of its length $F = 2\kappa l_2 \sin(\varphi/2)$ is defined by the formula of Stokes-Oseen [17]:

$$F = 4\pi\mu_V V_V \cdot (\ln(7.406 \cdot R_e^{-1}))^{-1},$$ (7)

where κ is the stiffness coefficient of the copper probe, φ is the angle of probe deflection (degree), μ_V is the coefficient of water dynamic viscosity, $R_e = \rho V_V d_{pr} \mu_V^{-1}$ is the Reynolds number. The stiffness coefficient of the

Fig. 11. The position of the probe before immersion in oil
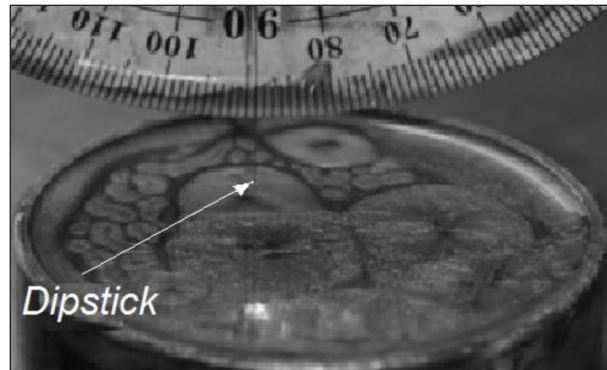
Fig. 12. The position of the probe after immersion in oil

Table 2. **Calibration data (table) on measurement of the probe deflection angle in water flow**

No.	Mass of water, M, ml	Time, t, sec	Angle of deflection, φ, degree	Diameter of jet, d, mm	Velocity of water, V, cm/sec
1	6	10	2	1.5	0.34
2	40	10	4	2.5	0.82
3	50	10	5	2.6	0.94
4	140	10	9	3	1.98

copper probe κ weakly depends on temperature (decreases linearly with the increase of temperature) in the range from room temperature to 500 °C [16].

Therefore, the ratio of stiffness coefficients of the copper probe at room temperature κ_V and oil temperature κ_{Oil} is assumed about one, i. e. $\kappa_V \kappa^{-1}_{Oil} \approx 1$.

Using the experimental data from Table 2, and considering the fact that the coefficient for transfer of water velocity in oil is determined by the value $V_V/V_{Oil} = \mu_{Oil}\kappa_V/(\mu_V\kappa_{Oil}) \approx 10.0$, a dependence graph of the convective velocity of oil on the wire deflection angle is constructed.

Figure 13 shows the calibration dependence of the wire deflection angle from the velocity of water, constructed to determine the velocity of oil in a cell.

As it follows from this figure, the oil flow velocity on the surface of a convective cell at a distance half of the radius from its axis is about $V_{Oil} \approx 0.2$ mm/sec.

The velocity of oil in a convective cell was also measured visually, using a microscope MBS-9. Aluminum powder concentration in oil was 29 mg/ml. The depth of the oil layer was 1 mm, the diameter of the container with oil was 5.2 cm. Velocity was measured in the following way. The container with convective cells was placed in the microscope instead of a glass slide so that the surface area of oil was orthogonal to the optical axis of the microscope optical head. A camera was fixed instead of an eyepiece. It fixed the video of marker movement (of the selected aluminum particle of the plate form) from the cell center to its periphery. Figure 14 shows markers with arrows. The frame-by-frame analysis of the video of markers allowed the estimation of their instantaneous velocity. Analyses of a set of experimental data of marker instantaneous velocities allowed determining the maximum radial velocity of oil.

Calculation of instantaneous velocity of markers showed that it undergoes random changes.
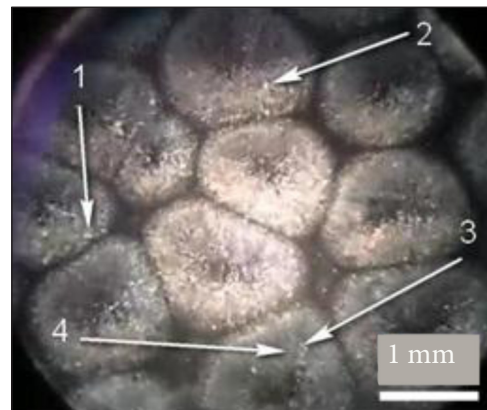
Fig. 14. Type of convective cells and position of markers
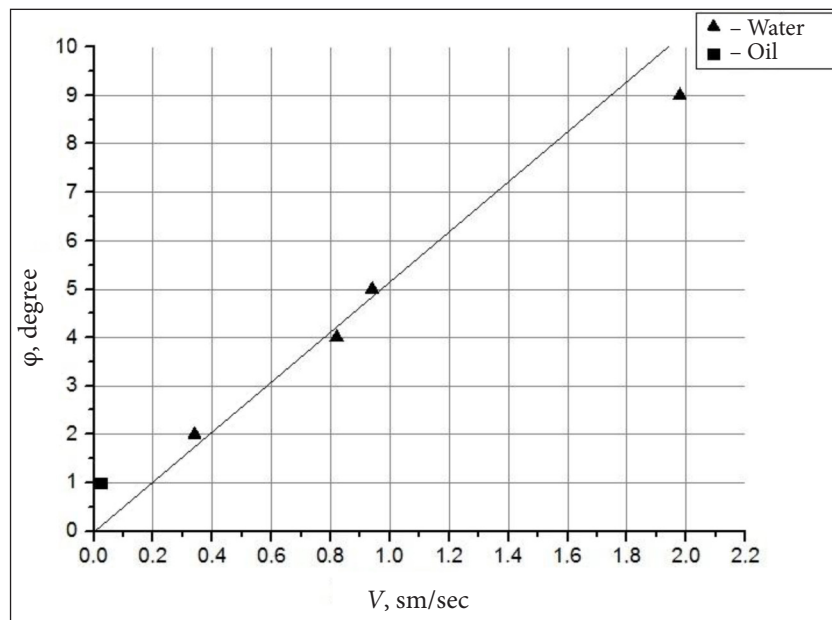
Fig. 13. Dependence of calibration of the wire deflection angle on the velocity of water

These changes are due to the rotation of markers in a stream of oil carrying them, which is characterized by the presence of the velocity gradient in the direction, which is perpendicular to the flow of traffic [15]. Rotation of marker changes the force of carrying it along the flow. Therefore, the resulting dependence of radial velocity of a particle on the radius was estimated on the envelopes of experimental points of instantaneous velocity. The envelopes are constructed in accordance with an analytical expression of the dependence of radial velocity on the cell radius (2).

Figure 15 shows the values of radial velocities of particles in black squares, depending on their position relatively to the center of a convective cell (in relative units). Curves, enveloping the experimental points in Fig. 15, determine

the dependence of radial velocity of a convective motion of oil on the radius. As a result of such constructions, one can conclude that the maximum radial velocity of oil in convective cells 1–4 amounts to 3.5–5.2 mm/sec.

Thus, it was shown in this part of the work that the velocity of mass transfer in a convective cell depends on dimensions of the cell and may be of the order of 4.35 mm/sec.

CONCLUSIONS

This work substantiates the existence of an elementary convective cell by comparing the theoretical model and experimental data. The characteristic velocities of fluid convection within a cell were obtained experimentally.
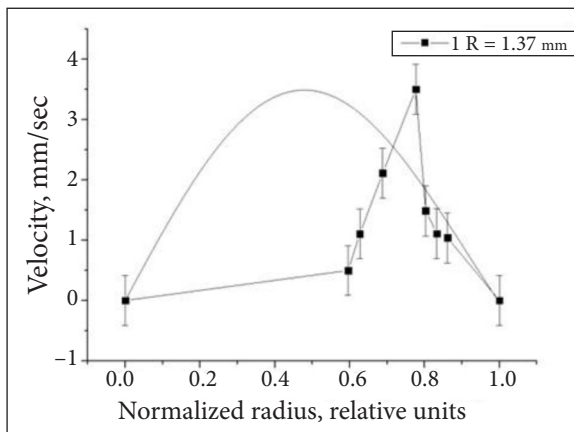
Fig. 15.1. Values of horizontal velocities of the particle for different values of the cell $R = 1.37$ mm
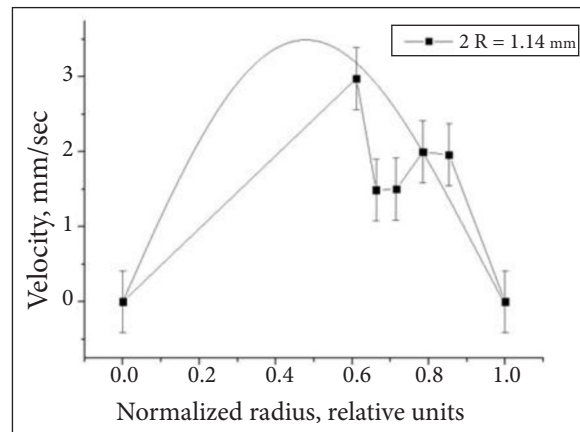
Fig. 15.2. Values of horizontal velocities of the particle for different values of the cell $R = 1.14$ mm
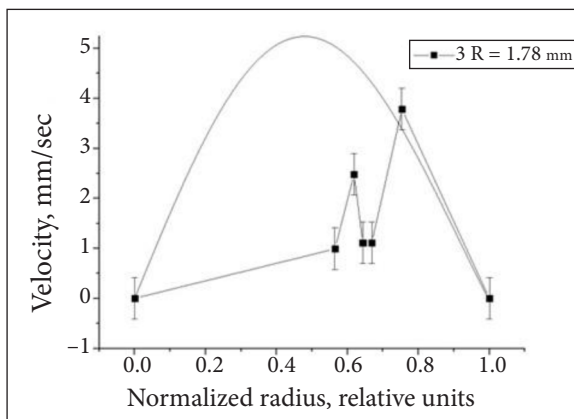
Fig. 15.3. Values of horizontal velocities of the particle for different values of the cell $R = 1.78$ mm
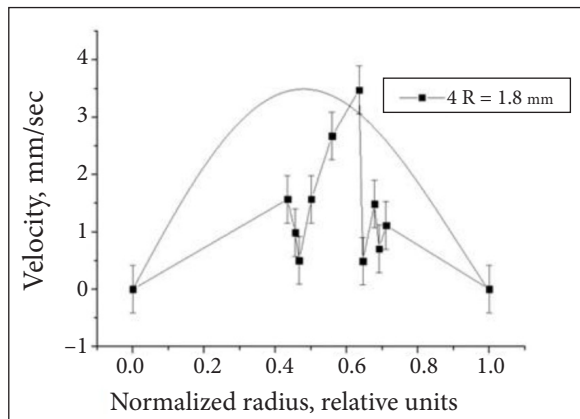
Fig. 15.4. Values of horizontal velocities of the particle for different values of the cell $R = 1.8$ mm

It was assumed that suspension near the bottom of the vessel should be regarded as separate environment with distinct density and viscosity compared with that of the pure oil. It moves along the bottom layer of pure oil without friction. It allows considering boundary conditions of the fluid layer as free. This assumption is supported by the results of numerical processing of the experimental data on formation of convective rings on the surface of fluid, heated from below, obtained by other authors.

As a result of the experiments on formation of a cylindrical convective cell by the overlay of the copper ring on the surface of oil, a qualitative and quantitative correspondence of the theoretical model to the experimental data was shown.

Velocity of the horizontal flow of oil on the surface of a convective cell with a diameter of 17 mm was determined in accordance with the angle of deflection of the movable probe. Its value is equal to $V_{Oil} \approx 0.02$ cm/sec. For cells with a smaller diameter (2 mm), the horizontal velocity of oil on the surface of a cell was measured by the optical method, and it equals 3.5–5.2 mm/sec.

References

1. Bernard H. Les tourbillons cellulaires dans une nappe liquid. *Revue generale des sciences, pures et appliques.* 1900. Vol. 11. P. 1261–1271 and 1309–1328.

2. Ray1eigh O. M. 412. On convection currents in a horizontal layer of fluid, when the higher temperature is on the underside. *Philosophical Magazine.* 1916. Vol. 32. P. 529–546.

3. Chandrasekhar S. *Hydrodynamic and Hydromagnetic Stability*. 1970. 657 p.

4. Gershuny G. Z., Zhuhovickiy E. M. *Convective Stability of Incompressible Fluid*. Moskva: Nauka, 1972. 393 p.

5. Getling A. V. *Rayleigh-Benard Convection. Structures and Dynamics.* Advanced Series in Nonlinear Dynamics. Vol. 11. 2001. 245 p.

6. Getling A. V. Formation of spatial structures of Rayleigh-Benard convection. *Uspechi fizicheskich nauk.* 1991. Vol. 161. No. 9. P. 1–80.

7. http://tavot-spb.ru/vakuumnye_masla

8. *Royal Society Mathematical Tables. Volume 7. Bessel Functions. Part 3. Zeros and Associated Values.* Cambridge: Cambridge University Press, 1960.

9. Koschmieder E. L. *Bénard Cells and Taylor Vortices (Cambridge Monographs on Mechanics).* Cambridge University Press, 1993. 350 p.

10. Zierep J. Über rotationssymmetrische Zellularkonvektionsströmungen. *Zeitschrift für Angewandte Mathematik und Mechanik.* 1958. Vol. 39. No. 7/8. P. 329–333.

11. Zierep J. Eine rotationssymmetrische Zellularkonvektions Strömung. *Beitraege zur Physik der Atmosphaere.* Vol. 30. P. 215–222.

12. Pavlov V. N., Kruzhanovskiy A. S. *Study of the Formation of Lubricating Layers in the Gearing. Problems of Friction and Wear.* Kiev: Technique, 2009. P. 183–186.

13. Khodakov G. S. The rheology of suspensions. Phase flow theory and its experimental validation. *Russian Chemical Journal.* 2003. Vol. 47. No. 2. P. 33–44.

14. Makarov M. A., Pyshnograi I. G., Pyshnograi G. V., Altukhov Y. A., Golovichёva I. E., Tregubova Y. B., Tretyakov I. V., Afonin G. L., A. L. Joda H. N. A. Statement of mesoscopic boundary conditions for the slip velocity at the boundary. *Polzunov Gazette.* 2012. No. 3/1. P. 61–74.

15. Batchelor J. *Introduction to Fluid Dynamics.* Mir, 1973. 792 p.

**Liudmyla Bozbiei, Boris Borts, Yuri Kazarinov,
Andrey Kostikov, Viktor Tkachenko**

**EKSPERIMENTINIS SKYSČIO JUDĖJIMO
LAISVOSE ELEMENTARIOSIOSE
KONVEKCIJOS LĄSTELĖSE TYRIMAS**

Santrauka

Elementariosios konvekcijos ląstelės (EKL) formuojamos horizontaliuose iš apačios šildomo skysčio sluoksniuose, jos eksperimentiškai tiriamos straipsnyje pristatytame darbe. Eksperimentinių tyrimų rezultatai aprašyti teoriniu EKL modeliu. Parodoma, kad pridėjus aliuminio miltelių į alyvą ji paverčiama suspensija, o ribinės sąlygos ant kietos sienelės gali būti laikomos laisvomis, kadangi yra slydimas grynosios alyvos juosta. Ribinių sąlygų pobūdžio kitimas patvirtinamas kitų autorių eksperimentiniais konvekcijos žiedų ant sluoksnio paviršiaus formavimo skaitmeninio apdorojimo rezultatais. Straipsnyje aprašyti du nepriklausomi metodai masės mainų greičiui skirtingo skersmens ląstelėse nustatyti. Maksimalus didelio skersmens ląstelių (17 mm) masės mainų greitis buvo matuojamas ties viršutine riba ant zondo nuokrypio kampo. Išmatuotas tokiu būdu greitis lygus $V_{Oil} \approx 0{,}2$ mm/s. Mažesnio skersmens ląstelių (2 mm) alyvos greitis ant ląstelės paviršiaus buvo matuojamas pasitelkus optinį metodą gauta reikšmė nuo 3,5 mm/s iki 5,2 mm/s.

    Raktažodžiai: elementariosios konvekcijos ląstelės, konvekciniai procesai, šilumos mainai, temperatūros gradientas, masės mainų ląstelėje greitis